Particle Morphology and NMR Structure of Polymethylmethacrylate/Polystyrene Emulsifier-Free Core–Shell Cationic Latices in the Presence of DBMEA

Jinzhi Zhang, Xiaoqin Li, Shigan Chai, Shimin Wang, Shiyuan Cheng

Faculty of Chemistry and Material Science, Hubei University, Wuhan 430062, China

Received 4 May 2004; accepted 4 October 2004
DOI 10.1002/app.21599
Published online in Wiley InterScience (www.interscience.wiley.com).

ABSTRACT: In the absence of emulsifier, we prepared stable emulsifier-free polymethylmethacrylate/polystyrene (PMMA/PSt) copolymer latex by batch method with comonomer *N*,*N*-dimethyl, *N*-butyl, *N*-methacryloloxylethyl ammonium bromide (DBMEA) by using A1BN as initiator. The size distribution of the latex particles was very narrow and the copolymer particles were spherical and very uniform. Under the same recipe and polymerization conditions, PMMA/PSt and PSt/PMMA composite polymer particle latices were prepared by a semicontinuous emulsifier-free seeded emulsion polymerization method. The sizes and size distributions of composite latex particles were determined both by quasi-elastic light scattering and transmission electron microscopy (TEM). The effects of feeding manner and staining agents on the morphologies of the composite particles were studied. The results were as follows: the latex particles were dyed with pH 2.0 phosphotungestic acid solution and with uranyl acetate solution, respectively, revealing that the morphologies of the composite latex particles were obviously core–shell structures. The core–shell polymer structure of PMMA/PSt was also studied by ^{1}H, ^{13}C, 2D NMR, and distortionless enhancement by polarization transfer, or DEPT, spectroscopy. Results showed that PMMA/PSt polymers are composed of PSt homopolymer, PMMA homopolymer, and PMMA-*g*-PSt graft copolymers; results by NMR are consistent with TEM results. © 2005 Wiley Periodicals, Inc. J Appl Polym Sci 97: 1681–1687, 2005

Key words: emulsion polymerization; morphology; core–shell polymers; latices; NMR

INTRODUCTION

Composite latices with different types of particle morphologies can be of great use in the fields of plastic, paint, and coatings industrial applications.[1,2] Some of these applications involve enhancing the strength of adhesives, and modifying and enhancing the toughness of engineering plastics. They can also be used as water-resistant, radiation-resistant, invisible, and weather-resistant films.

Composite latex particles with different particle morphologies can be prepared by two-stage emulsion polymerization, seeded emulsion polymerization methods, equilibrium-swelling batch methods, and semibatch methods, to cite a few examples. When the second-stage monomer is different from the monomer of the seed polymer, phase separation occurs and many types of heterogeneous morphologies may be formed. Okubo and coworkers[3–6] showed that heterogeneous composite polymer particles could change the particle morphologies from confetti-like to raspberry-like and containing voids. The film-forming properties of latex depend on the particle morphologies and the surface properties, although the particle morphologies depend on the molecular weights of polymers, the internal particle viscosity during polymerization, polymerization condition, and the difference of the core–shell polymer in hydrophilicity and solubility, for example. In recent years, there have been some reports on emulsifier-free core–shell-structured emulsion polymerization.[7–10] However, these investigations were restricted with anion emulsion. In the present work, we primarily investigated the synthesis of styrene/methylmethacrylate/*N*,*N*-dimethyl, *N*-butyl, *N*-methacryloloxylethyl ammonium bromide (St/MMA/DBMEA) emulsifier-free cationic copolymer emulsion by the batch method and of MMA–St functional polymer latices with core–shell morphologies by the semicontinuous method, using DBMEA as comonomer. DBMEA provides cationic  quaternized groups in the surface of the particles. The morphologies of latex particles were investigated in detail with pH 2.0 phosphotungestic acid (PTA) and uranyl acetate (UAc) as staining agents, and the core and shell structures of the composite latex particles can clearly be seen.

Two-dimensional (2D) NMR techniques have been applied to vinyl and related polymers. For example,

Correspondence to: S.-Y. Cheng (scheng@public.wh.hb.cn).

2D J-resolved proton spectroscopy and 2D techniques have been applied to polymers[11–13]: Macura and Brown[14] applied 2D J-resolved proton spectroscopy to poly(vinyl chloride); Bruch and Bovey[15] applied proton nuclear Overhauser effect spectroscopy (NOESY) to interpret the spectrum of a vinylidene chloride–isobutylede copolymer. Mao et al.[12] reported proton NOESY to study the stereochemical configuration of polymethylmethacrylate (PMMA)–naphthyl ethylene. Heffner et al.[11] described a study of the isotactic and atactic PMMA by NOESY and J-resolved 2D NMR. In this article, we apply carbon-13, proton, distortionless enhancement by polarization transfer (DEPT), gradient heteronuclear multiple quantum coherence (gHMQC), and NOESY to the further exploration of the structure of PMMA/polystyrene (PMMA/PSt) core–shell polymer.

EXPERIMENTAL

Materials

Styrene (St) was purified by distillation under vacuum and then stored in a refrigerator until required; methylmethacrylate (MMA) was washed with 10% aqueous sodium hydroxide purified by passing through the inhibitor-remover; azobis(isobutylamidine hydrochloride) [$(NH_2)_2C^+(CH_3)_2CN{=}NC(CH_3)_2C^+(NH_2)_2{\cdot}2HCl$] (AIBA) was kindly supplied by Institute of Chemical Engineering (Beijing, China) and used directly without further purification. Dimethylaminoethyl methacrylate (DMAEMA) and *N*,*N*-dimethyl, *N*-butyl, *N*-methacryloloxylethyl ammonium bromide [$CH_2{=}C(CH_3)COOCH_2CH_2N^+(CH_3)_2C_4H_9Br^-$] (DBMEA) was synthesized before use according to the method previously described in the literature[16,17] (yield: 92.51%, t_f 108–108.5°C). Double-distilled water was used in all experiments.

Synthesis of P(MMA/St/DBMEA) copolymer latices by batch method

Copolymer latices were prepared by the batch process, using the following recipe: St/MMA = 15 mL/15 mL; 2% DBMEA = 10 mL; the amount of AIBA should be 0.5 wt % of total monomer. Under the emulsifier-free condition, the polymerizations were carried out in a 250-mL glass reactor, equipped with a reflux condense, a stirrer, and a thermometer. All the ingredients and 130 mL deionized water were first charged and the reactor was heated to the required temperature before the addition of initiator solution. The polymerization was carried out under an inert nitrogen atmosphere and in a thermostat water bath at about 74 ± 0.5°C. The reaction was maintained for 5 h and then cooled to ambient temperature.

Synthesis of seed latices by batch method

Under the emulsifier-free condition, we first synthesized seed polymer latices by the batch method. The recipe is as follows: MMA = 15 mL (or St = 15 mL); 2% DBMEA = 5 mL; the amount of AIBA was 0.5 wt % of MMA (or St) monomer. The preparation process was similar to the synthesis of P(MMA/St/DBMEA) copolymer latices by the batch method.

Synthesis of composite latices by semicontinuous polymerization method

After synthesis of seed polymer latices, the reaction temperature was kept at about 74 ± 0.5°C. A mixture of 5 mL 2% DBMEA and 0.5 wt % of shell monomers was added to the seed latex and 15 mL shell monomers was added to the reactor in a dropwise manner at a drip rate of 0.25 mL/min. When the dropwise addition was completed, the reaction temperature was kept at about 74 ± 0.5°C for 5 h after which it was cooled to ambient temperature.

Particle size and morphologies

The particle size was measured by quasi-elastic light scattering (QELS), and polydisperity index values were obtained. Latex particle morphologies were observed by transmission electron microscopy (TEM). First, a certain quantity of emulsion was diluted properly by distilled water and then stained with pH 2.0 (or pH 6.4) phosphotungestic acid (PTA) solution and uranyl acetate (UAc) solution, respectively. The mixture was allowed to stand for a while, and after filming on copper, the sample was dried at room temperature. TEM was performed by use of a TEM-100SX instrument (JEOL, Tokyo, Japan). The particle size was determined by TEM. The particle diameters, from 100 to 150 particles, were measured and the values averaged in each sample.

Stability of latex

The final latex was stored at room temperature for 15 months under a sealing condition. The changes in emulsion showed the storage stability.

NMR measurements

The 600-MHz ^{1}H-NMR and 150-MHz ^{13}C-NMR spectra were recorded on a Inova-600 spectrometer (Varian Associates, Palo Alto, CA). The polymer solutions were prepared with $CDCl_3$ as lock and Me_4Si (TMS) as internal reference. The solution concentrations were about 10% (w/v) for the proton and carbon experiments.

TABLE I
Size and Distribution of P(MMA/St/DBMEA) Copolymer Latex Particles by QELS and TEM

	QELS		TEM	
Latex	D_w (nm)	Poly	D_w (nm)	Peak number
P(MMA/St/DBMEA)	328.5	0.013	250.2	single peak

Phase-sensitive NOESY spectra were recorded at room temperature. The processed data matrix consisted of 1024 × 1024 points. The mixing time was 0.6 s with eight scans collected for each of the 256 spectra. The processed matrix 0.0836 × 0.011 Gauss function was applied in the phase-sensitive spectra.

RESULTS AND DISCUSSION

Copolymer latex of emulsifier-free P(MMA/St/DBMEA)

Particle size and distribution of final latices, as obtained by TEM and QELS, are reported in Table I. It is worth noting that all the particle sizes measured by TEM appear to be generally smaller than the corresponding sizes determined by QELS (as seen Tables I, II, and III); the larger sizes obtained by QELS are possibly attributable either to the presence of an immobilized water layer surrounding the particles in the aqueous medium or to swelling of the latex particles and the charged colloidal particles with the double electrical layer. In addition, particles under the electron beam might be subjected by some shrinkage of the dried particles.

The results shown in Figure 1 indicate that the copolymer particles were spherical and of very narrow particle size distributions (PSD) by TEM observation. Results from QELS, as shown in Table I, show that the distributions of copolymer latex particles produced only a single peak; the mean diameter (D_w) and the polydispersity index (poly) value were 328.5 nm and 0.013, respectively. Furthermore, the smaller poly shows that the distributions of P(MMA/St/DBMEA) particles were monodisperse. These phenomena may be explained by the fact that all the nucleation stage of latex particles is completed at about 10% conversion in emulsifier-free emulsion polymerization; the nucleation period of particles is much earlier than that in conventional emulsion polymerization, in which the nucleation stage usually ends at about 15–25% conversion.[18]

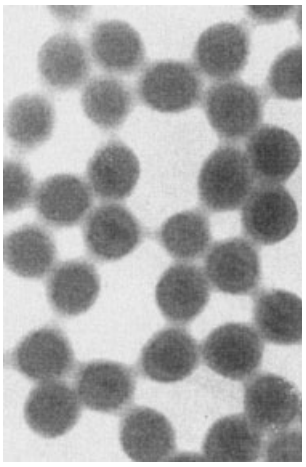

Figure 1 TEM microphotographs of the soap-free P(MMA/St/DBMEA) copolymer particles by batch emulsion polymerization method.

TABLE II
Comparison of Different Staining Methods Used in TEM for Latices PSt and PMMA Seed Latex Particles

	TEM		QELS	
	pH 2.0 PTA	UAc	No staining	
Seed latex	D_w (nm)	D_w (nm)	D_w (nm)	Poly
PS	125.3	128.5	157.8	0.0502
PMMA	158.1	168.7	226.3	0.164

Seed emulsion polymerization

The first stage in the preparation of the desired core–shell polymer latex was the synthesis of monodisperse seed latex to obtain the ultimate core–shell polymer colloid with a well-defined shape.

As seen Table II, the seed latex particles of PSt or PMMA were prepared by the batch method in the absence of emulsifier. The size distributions of the two seed latex particles were very narrow. As seen in Figure 2, two seed latex particles are spherically shaped with a smooth particle surface and a monodisperse PSD after the latex particles were dyed with pH 2.0 PTA solution and with UAc solution, respectively. Moreover, both staining agents gave similar results. There were no significant differences in particle diameters and morphologies for the same sample between using pH 2.0 PTA and UAc agent: both particles had a well-defined and spherical shape. This likely was because both pH 2.0 PTA and UAc stained with cationic quaternized groups and amidine groups on the surface of the particles, and thus the color seemed darker on the outer latex particle.

Morphologies of PSt/PMMA emulsifier-free latex particles

Under the same recipe and polymerization conditions, the only difference between P(MMA/St/DBMEA) and PSt/PMMA was the feeding method: PSt/PMMA emulsifier-free latex was prepared using the PSt as

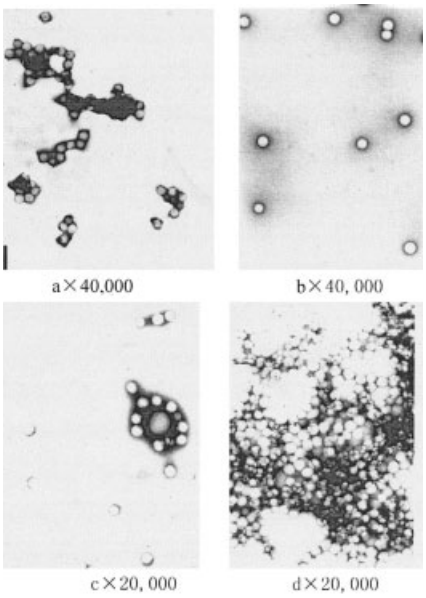

Figure 2 TEM microphotographs of the seed polymer particles by batch emulsion polymerization method: (a) PSt with pH 2.0 PTA staining; (b) PSt with UAc staining; (c) PMMA with pH 2.0 PTA staining; (d) PMMA with UAc staining.

seed latex particles and MMA was used as the second-stage monomer by semicontinuous monomer in a dropwise manner. To enhance the contrast behavior of the phase components of particles, pH 6.4 and pH 2.0 PTA and UAc, respectively, were used as staining agents in the TEM micrographs of the final latex particles for the PSt/PMMA. Figure 3(a) and (b) show the effects of the different staining techniques for the same sample. By comparing Figure 3(a) and (b) to Figure 2(a) and (b), the core and shell structures of the composite latex particles can be seen clearly by use of pH 2.0 PTA and UAc staining; PSt seed particles (darker gray area) appear to be almost covered by the PMMA second stage (lighter gray area) polymer. In fact, the regions stained by pH 2.0 PTA and UAc were the surface layer of the particles and the layer between the core and shell, containing bonded cationic quaternized groups and amidine groups.[19]

In the semicontinuous process, the second-stage monomer was gradually added to the first-stage seed particles. The second-stage monomer contents were kept so low on the surface of the core phase that they were under starved conditions; thus semicontinuous polymerization was used to improve the formation of the core–shell structure latex, so that the latex particles formed a clear and orbicular core–shell structure, obtaining better distribution of the shell polymer based on the seed latex particles. However, we have found that the PSt/PMMA composite latex particles did not exhibit a core–shell structure with pH 6.4 PTA staining; moreover, some latex particles coagulated (see figure sketch), which may be because the pH 6.4 PTA could neutralize cationic ion groups on the surface of the latex microspheres, thus promoting some coagulation. Therefore these results indicate that the characterization of composite particle morphologies depends on not only the monomer feeding method but also the selected staining reagent; thus pH 6.4 PTA staining agent is not suitable for use with the emulsifier-free cationic emulsion.

Morphologies of PMMA/PSt emulsifier-free latex particles

Under the sample recipes conditions, varying only the feeding sequence of the main monomer MMA and styrene, PMMA/PSt composite latex particles were prepared using the PMMA seed latex particles and styrene was used as the second-stage monomer. The same PMMA/PSt sample was stained with pH 2.0 PTA and UAc solution, respectively, as seen in Figure 3(c) and (d) and Table III. By comparing Figure 3(c) and (d) to Figure 3(a) and (b), it was found that PMMA/PSt composite latex had narrower PSDs and the core–shell structures are clearer and diameters are larger than those of PSt/PMMA. The particles in Figure 3(a) and (b) were deformed and nonspherical be-

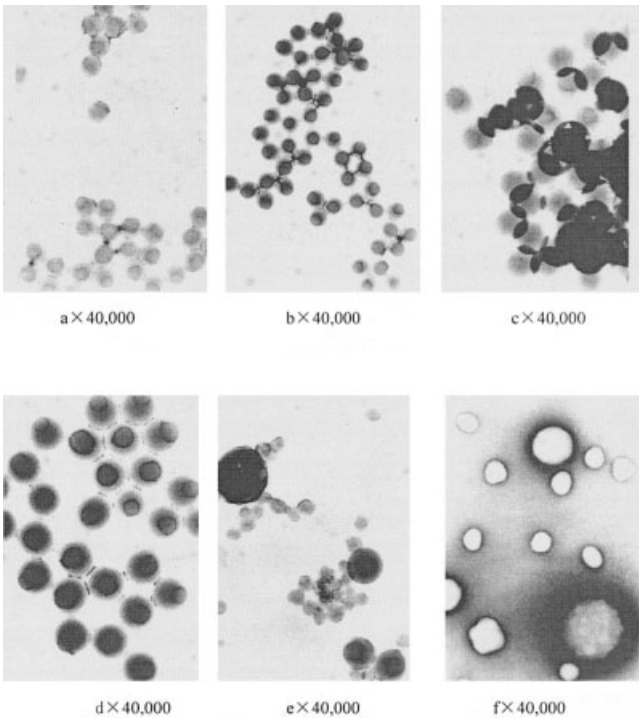

Figure 3 TEM microphotographs of composite particles by semicontinuous polymerization method: (a) PSt/PMMA with pH 2.0 PTA staining; (b) PSt/PMMA with UAc staining; (c) PMMA/PSt with pH 2.0 PTA staining; (d) PMMA/PSt with UAc staining; (e) PMMA/PSt with emulsifier with pH 2.0 PTA staining; (f) PMMA/PSt with emulsifier with UAc staining.

TABLE III
Comparison of Different Staining Methods Used in TEM for Core/Shell Latex Particles and Comparison of TEM and QELS Methods for Composite Latex Particles

	TEM		QELS	
	pH 2.0 PTA	UAc	No staining	
Core–Shell latex	D_w (nm)	D_w (nm)	D_w (nm)	Poly
PSt/PMMA	148.8	147.5	193.5	0.113
PMMA/PSt	223.5	216.4	293.6	0.106
PMMA/PSt (with emulsifier[a])	139.4	132.7	177.3	0.246

[a] Emulsifier: $C_{16}H_{31}N^+(CH_3)_3Br^-$.

cause the outer PMMA polymer is only weakly affected by electron beams; the PMMA/PSt latex particles do not easily deform in the electron beam and the shape of PMMA/PSt latex particles are very uniform. Moreover, as seen in Tables III and I, the smaller poly values show that both the seed and the composite particles were monodisperse; the results are in substantial agreement with those of TEM.

As seen in Figure 3(c) and (d), both staining methods gave similar results: PMMA/PSt composite particle morphologies are of obvious core–shell structures, the size distribution of latex particles were uniform, and there were no significant differences between the average particle diameters determined by the two staining methods. It is assumed that quaternized groups and amidine groups are both assimilated on the surface of the seed particles. The AIBA initiator is soluble in aqueous media and its reactions are mainly present in the aqueous phase. The amidine radical exists near the surface of the particles and, because of the stable seed latex particles, the mobility of the radical was restricted, resulting in increased time required for the growing radical to diffuse into the interior of the particle. The high viscosity inside the particle, as well as the anchoring of the growing radical by polymerizing with the vinyl groups of the shell monomer, excluded reaction loci in the inner regions. Therefore, the second polymerizations occurred mainly in the shell region of the latex particles. In addition, the hydrophilic and the immiscibility between the PMMA and PSt polymers resulted in core–shell phase separation and the shell polymers were excluded from the exterior of the seed particles, making regular domains and forming an obvious core–shell structure.

Under the same polymerization conditions, by adding only a small quantity of cationic emulsifiers in the second phase, as seen in Figure 3(e) and (f), some latex particles of core–shell can be distinguished (others are invisible). Moreover, by comparing Figure 3(c) and (d) to Figure 3(e) and (f), it was found that the sizes of PMMA/PSt latex particles became a multimodal PSD, consisting of very small particles (<100 nm) and larger agglomerated particles; the average diameter of PMMA/PSt particles is smaller than that of PMMA seed latex particles [see Table III and Fig. 3(e) and (f)]. Because of the addition of emulsifier, which produces secondary micelles, and the formation of secondary particles, in the PMMA-rich seed region, some polymerizing reactions on PMMA particles could form larger PMMA/PSt core–shell particles; however, others could not migrate onto the PMMA surface region, resulting in the formation of isolated new PSt latex particles, although the new latex particles produced from the second stage are very small. Thus both the smaller-diameter secondary particles and the larger core–shell particles coexist simultaneously in the polymerization process, that is, there is a dual particle-nucleation mechanism with multimodal broad particle size distributions.

Stability of the MMA–St emulsifier-free latex

During the entire latex polymerization process, no coagulates were formed; and when the latices had been stored for 15 months at room temperature, no precipitates were produced. These experimental results showed that latices prepared by emulsifier-free emulsion polymerization were quite stable because, when the polymerization was carried out, DBMEA could be bonded onto the surface of the latex particles, provided the $CH_2{=}C(CH_3)COOCH_2CH_2N^+(CH_3)_2C_4H_9$ cationic quaternary ammonium groups acted as surfactant, or DBMEA could be polymerized in the water phase, acting as polyelectrolyte hydrosoluble chains. Therefore surface-charge densities of the latex particle could be greatly improved, thus leading to stable latices. On the other hand, AIBA also significantly improved the stability of the latices. The end groups of $-C(CH_3)_2C^+(NH_2)_2$ on the particle surfaces acted as surfactants to increase electrostatic repulsion and therefore the latex particles would be stabilized.

NMR spectroscopy of PMMA/PSt

Figures 4, 5, and 6 show the 600-MHZ proton [Fig. 4(a)], carbon [Fig. 4(b)], DEPT [Fig. 4(c)], 2D gHMQC (Fig. 5), and 2D NOESY (Fig. 6) spectra of PMMA/PSt core–shell polymers. The spectra by ^{13}C and DEPT revealed the phenyl –CH (~ 125.4–127.7 ppm), quaternary C(St) (~ 143.5 ppm), styrene α-CH (~ 51.7 ppm), β-CH_2(St) (~ 44.9 ppm), carbonyl signals (MMA) (~ 176.6 ppm), quaternary α-carbon (MMA) (~ 44.6 ppm), β-CH_2(MMA) (~ 52.0–54.1 ppm), $-OCH_3$ (~ 51.5 ppm), and α-CH_3 (~ 16.3 and 18.5 ppm).[11–13] The spectra by ^1H and gHMQC spectra revealed the phenyl group (~ 6.4–7.1 ppm), styrene β-CH_2(St) (~ 1.4 ppm), styrene α-CH (~ 1.8 ppm),

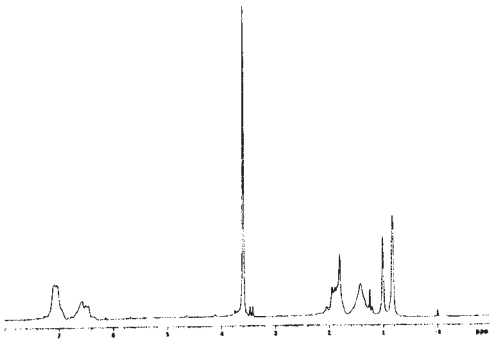

4(a). 600MHz1H spectrum

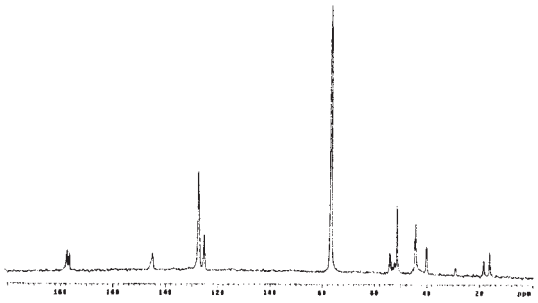

4(b) 150Mhz carbon-13 spectrum

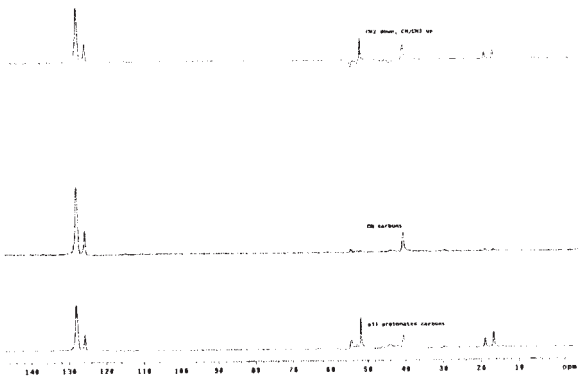

4(c) 150Mhz carbon-13 DEPT

Figure 4 NMR spectra of PMMA/PSt core–shell polymer: (a) 600-MHz ^{1}H spectrum; (b) 150-MHz ^{13}C spectrum; (c) 150-MHz ^{13}C DEPT.

α-CH_3 ($\sim$ 0.84 and 1.02 ppm,), OCH_3 ($\sim$ 3.6 ppm), and β-CH_2 ($\sim$ 1.85–2.06).

Figure 6 shows the 600-MHZ proton NOESY spectrum of the core–shell polymer, observed under the same conditions as those in Figure 4(a). The spectrum

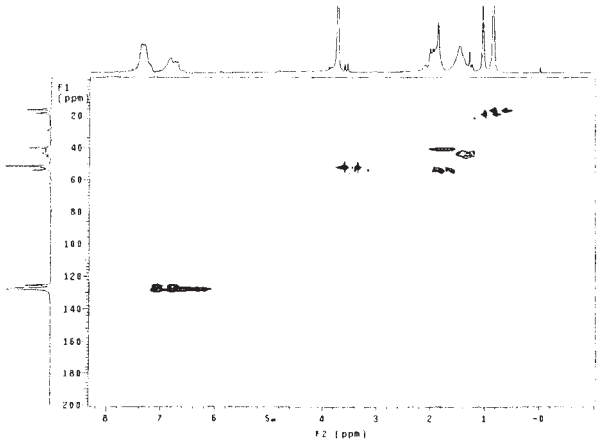

Figure 5 gHMQC spectrum of PMMA/PSt polymer.

is presented in the phase-sensitive mode. Assignments between the aliphatic α-CH_3 (upfield) and aromatic (6.4 ppm) indicated that cross-peaks are not observed, but the cross-peaks are observed between aromatic aromatic (6.4 ppm) and α–CH(St), between aromatic aromatic (6.4 ppm) and β-CH_2(St), respectively; these results confirm the existence of homopolymer PSt in the core–shell PMMA/PSt polymer; of course, there is also homopolymer PMMA. The results are consistent with core–shell morphologies and phase separation by TEM. However, β-CH_2(St) resonance exhibits NOE cross-peaks to the region of the β-CH_2(MMA) resonance; no doubt the results confirm the existence of PMMA-*g*-PSt graft copolymers in the PMMA/PSt core–shell polymer.[20]

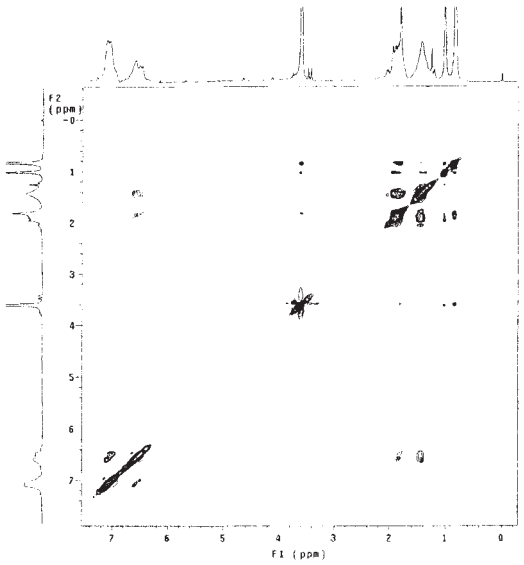

Figure 6 Proton phase-sensitive NOESY spectrum (600 MHz) of PMMA/PSt core–shell polymer. The mixing time was 600 ms.

CONCLUSIONS

Emulsifier-free emulsion polymerization with cationic comonomer DBMEA, under batch conditions, resulted in monodisperse latices, such as P(MMA/St/DBMEA) copolymer latex and seed polymer latex.

Under the same recipe and polymerization conditions, PSt/PMMA and PMMA/PSt emulsifier-free composite latex were prepared by semicontinuous monomer in a dropwise manner. Latex particles were clearly shown to have core–shell morphologies with pH 2.0 PTA and UAc staining, although the latex particles were shown to coagulate with pH 6.4 PTA staining; thus the cationic emulsion may not use pH 6.4 PTA staining. In addition, particle size measurements may give larger diameters by QELS than by TEM; the diameters revealed by QELS may be caused by swelling and formation of a double electrical layer. Under the same polymerization conditions, a small quantity of cationic emulsifiers caused PMMA/PSt latex particles to form multimodal particle size distribution with smaller diameter and the growth of core–shell particles; thus in the polymerization process, there can be a dual particle-nucleation mechanism. The core–shell polymer structure of PMMA/PSt was also studied by NMR spectroscopy. Results show that PMMA/PSt polymers are composed of PSt and PMMA homopolymers and PMMA-*g*-PSt graft copolymers; results by NMR are consistent with TEM studies.

References

1. Ji, Q. X.; Cheng, S. Y.; Li, J. Z. Polym Mater Sci Eng 1994, 2, 9.
2. Hirose, M.; Kadowaki, F.; Zhou, J. Prog Org Coat 1997, 31, 157.
3. Okubo, M.; Yamada, A.; Matsumoto, T. J Polym Sci Polym Chem Ed 1980, 16, 3219.
4. Okubo, M.; Ando, M.; Yamada, A.; Katsuta, Y.; Matsumoto, T. J Polym Sci Polym Lett Ed 1981, 19, 143.
5. Okubo, M.; Katsuta, Y.; Matsumoto, T. J Polym Sci Polym Lett Ed 1980, 18, 481.
6. Okubo, M.; Katsuta, Y.; Matsumoto, T. J Polym Sci Polym Lett Ed 1982, 20, 45.
7. Guo, T. Y.; Tang, G. L.; Hao, G. J.; Song, M. D.; Zhang, B. H. J Appl Polym Sci 2002, 86, 3078.
8. Lin, K. F.; Shieh, Y. D. J Appl Polym Sci 1998, 69, 2069.
9. Hu, R.; Dimonie, V. L.; El-Aasser, M. S. J Appl Polym Sci 1997, 64, 1123.
10. Chen, S. A.; Lee, S. T. Macromolecules 1991, 24, 3340.
11. Heffner, S. A.; Verge, L. A.; Mirau, P. A.; Tonelli, A. E. Macromolecules 1986, 19, 1628.
12. Mao, S. Z.; Yuan, H. Z.; Feng, H. Q. Chin J Magn Reson 1997, 14, 236.
13. Voronov, S.; Tokarev, V.; Datsyuk, V.; Seredyuk, V.; Bednarska, O. J Appl Polym Sci 2000, 76, 1228.
14. Macura, S.; Brown, L. R. J Magn Reson 1983, 53, 529.
15. Bruch, M. D.; Bovey, F. A. Macromolecules 1984, 17, 978.
16. Zhang, J.-Z.; He, X.-J.; Li, X.-Q.; Cheng, S.-Y. Chin J Colloid Polym 2003, 21, 10.
17. Huang, S.; Xu, Z.; Chen, Z.; Zhang, J. Chem Adhes 1997, 3, 128 (in Chinese).
18. Cheng, S.; Li, J.; Ji, Q. Polym Bull 1991, 3, 129.
19. Zhang, J.-Z.; Cheng, S.-Y.; Li, X.-Q. Polym Mater Sci Eng 2002, 18, 70 (in Chinese).
20. Min, T. I.; Klein, A.; El-Aasser, M. S.; Vanderhoff, J. W. J Appl Polym Sci 1983, 21, 2845.